IEEE Access
Multidisciplinary | Rapid Review | Open Access Journal

Received April 12, 2018, accepted May 18, 2018, date of publication May 28, 2018, date of current version June 19, 2018.

Digital Object Identifier 10.1109/ACCESS.2018.2841055

Fabric Defect Detection Based on Biological Vision Modeling

CHUNLEI LI[1], GUANGSHUAI GAO[1,2], ZHOUFENG LIU[1], MIAO YU[1], AND DI HUANG[2]
[1]School of Electronic and Information Engineering, Zhongyuan University of Technology, Zhengzhou 450007, China
[2]School of Computer Science and Engineering, Beihang University, Beijing 100191, China

Corresponding author: Chunlei Li (lichunlei1979@sina.com)

This work was supported in part by the National Natural Science Foundation of China under Grants 61772576 and 61379113, in part by the Key Natural Science Foundation of Henan Province under Grant 162300410338, in part by the Science and Technology Innovation Talent Project of Education Department of Henan Province under Grant 17HASTIT019, in part by the Henan Science Fund for Distinguished Young Scholars under Grant 184100510002, and in part by the Open Projects Program of National Laboratory of Pattern Recognition under Grant 201700015.

ABSTRACT Fabric defect detection plays a key role in the quality control of textiles. Existing fabric defect detection methods adopt traditional pattern recognition methods; however, these methods lack adaptability and present poor detection performance. Because biological vision system has the ability to quickly locate salient objects, we propose a novel fabric defect detection algorithm based on biological vision modeling by simulating the mechanism of biological visual perception. First, a distinct, efficient, and robust feature descriptor from the biological modeling of P ganglion cells, which was proposed in our previous work, is adopted to improve the representation of fabric images with complex textures. To account for the low-rank and sparsity characteristics of biological vision, the low-rank representation (LRR) technique is adopted to model biological visual saliency, and it can decompose the fabric image into backgrounds and salient defect objects. Meanwhile, dictionary learning and Laplacian regularization are integrated into the LRR model as follows: 1) dictionary learning is used to denoise the saliency map; and 2) Laplacian regularization enlarges the gaps between defective regions and the background. Finally, the linearized accelerated direction method with adaptive penalty is adopted to solve the proposed model. The experimental results emphasize that the proposed algorithm has good detection performance for plain or twill fabrics with simple textures as well as for patterned fabrics with complex textures. Moreover, the proposed method is superior to the state-of-the-art methods in terms of its adaptability and detection efficiency.

INDEX TERMS Fabric defect detection, biological vision modeling, image representation, dictionary learning, low-rank representation.

I. INTRODUCTION

Fabric defect detection plays a key role in the quality control of textiles and has historically been achieved via visual inspections by skilled workers. Thus, the detection performance depends on the experience and professional skills of the workers. Manual inspection methods have many disadvantages, such as high error rates because of human fatigue, high labor costs, and slow inspection speed. Moreover, the skilled inspection workers can detect only 15-20 meters per minute. To meet the requirement of industrial weaving, fabric defect detection based on machine vision has become a research focus.

Traditional fabric defect detection methods based on machine vision are mainly divided into two categories: detection methods for plain and twill fabrics, which include statistical analysis methods [1], model-based methods [2], spectral approaches [3] and dictionary learning-based methods [4]; and detection methods for patterned fabrics with complex textures, which include the wavelet-preprocessing golden image subtraction (WGIS) method [5] and ELO rating (ER) method [6]. The above two categories are designed for specific types of fabric images; however, they lack adaptability, and the detection performance is not ideal.

The biological vision system has the ability to rapidly locate salient objects. Although the texture of fabric images is complex, any type of defect is salient among the complex texture background. Therefore, fabric defect detection methods inspired by the biological vision system have been

a promising research field. Currently, researchers have proposed some defect detection methods based on the visual saliency model [7], [8]. Using these methods, low-level features are extracted, such as color, gradient, local texture and spectrum, and then the ''center-surround'' contrast and context analysis techniques are adopted to generate the saliency map. Finally, the defective regions can be located by adopting a threshold segmentation method. However, the techniques such as feature extraction and saliency calculation, still adopt traditional methods in pattern recognition. Therefore, these methods still perform poorly for fabric images with complex textures, and they cannot detect defects that present limited differences from the normal background.

In this paper, we establish a novel fabric defect detection framework inspired by the biological vision system, and it includes fabric image representation and saliency calculations. Considerable progress has been achieved in visual perception mechanism research, which shows that invariant feature extraction is one of the most important information processing tasks for the human visual system, and is also a common characteristic of senior cortex cells in the process of information integration. Therefore, the feature descriptors based on the mechanisms of the human visual system are more suitable for characterizing the complex textures of different fabric types. In previous work, we proposed an image descriptor with highly distinctive and robust and presented low complexity by modeling P retinal ganglion cells in human visual pathways [9]. This descriptor is suitable for describing all types of texture images and superior to the traditional hand-crafted feature descriptors. Therefore, it is adopted to characterize the fabric image texture in this paper.

At the saliency calculation phase, the low-rank representation model is consistent with the low-rank and sparsity features of the biological vision system. Therefore, this model is utilized to simulate visual saliency, and it can decompose the image into background and salient objects. Currently, the low-rank representation model has been used for object detection in natural scenes [10]. The background of a fabric image is redundant, while the defects are sparse among the background. Compared with object detection in a nature scene, fabric defect detection can better conform to the low-rank representation model. However, directly applying the available low-rank representation model for defect detection can produce results that are contaminated by noise, and this model may not be able to detect defects that present limited differences from the background.

Inspired by the hierarchical information processing mechanism in the biological vision system, we propose a novel fabric defect detection method based on biological vision modeling. First, we adopt the feature descriptor from the biological modeling of the P ganglion cells, which is proposed in our previous work to characterize fabric texture. Then, an improved low-rank representation model is proposed by introducing dictionary learning and Laplacian regularization to model visual saliency. The LADMAP method is utilized to solve the proposed model with high efficiency. Finally, an improved adaptive thresholding segmentation method is used to segment the saliency map generated by the sparse matrix to locate the defective regions.

II. RELATED WORKS

Current fabric defect detection methods can be divided into two categories according to the types of fabrics, with one category primarily focusing on plain or twill fabric images with simple textures and the other category focusing on patterned fabric images with complex textures. The proposed methods that focus on fabric images with simple textures include statistical analysis, model-based, spectrum analysis, and sparse representation approaches.

Statistical analysis methods divide the test image into image blocks. During the process of detection, the texture of the normal image blocks is assumed to have the same statistical properties and occupy most of the image. The image blocks with different statistical properties will be marked as defective regions. The representative methods include the differential counting box method [11], double-thresholding method [12], and histogram characters analysis method [13]. However, different statistical methods are suitable for specific fabric textures and may not be adaptable to various types of fabrics and defects.

The model-based methods model fabric texture as a stochastic process and the texture image can be regarded as a sample generated by the process in the image space. Defect detection is treated as a hypothesis test problem of statistical information derived from this model. The adopted models include the Gauss-Markov random field (GMRF) model [14] and Gaussian mixture model [15]. These methods usually have high computational complexity, and their detection results are not satisfactory for defects with small size. Spectral analysis methods transform the fabric images into the spectrum domain using Fourier transform [16], Gabor transform [17] and wavelet transform [18], and they then apply energy criteria for defect detection. Because these methods utilize the overall characteristics of the images to detect defects, they can achieve better detection performance for a fabric image with a simple texture. However, the computational complexity of these methods is high, and the detection results depend on the selected filter banks; thus, they have difficulty in detecting patterned fabric defects with complex textures.

Dictionary learning-based methods first learn a dictionary from the training images or test images, and then reconstruct the defect-free fabric image using the learned dictionary, thereafter, defect detection can be realized by subtracting the recovered image from the test image [19], [20]. In a different way, dictionary learning based methods also reduce the dimension of an image block by projecting the image block into a dictionary learning from reference image, then the support vector data description (SVDD) is adopted to discriminate whether an image block is a defect block [21]. However, if the dictionary is learned from the test images, the reconstructed images may exist some defects; or the self

adaptability of these methods are reduced if the dictionary learns from the reference images.

Although the aforementioned defect detection methods may achieve high detection accuracy for certain fabrics, because of the complexity and sophisticated design of patterned fabrics, these methods cannot be extended to detect patterned fabric defects. Certain methods for patterned fabric defect detection have been proposed, such as the wavelet-preprocessing golden image subtraction method (WGIS) [5], the Bollinger band method (BB) [22], the regular band method (RB) [23], template matching for discrepancy measures (TMPM) [24], the pattern matching and subtraction approach [25]–[28], the hash function method [29], the ELO rating (ER) method [6], and the low-rank recovery method [30].

The WGIS method selects a defect-free sample as a window, and the window size should be greater than the size of the repeated element of the fabric texture. The window is moved on a defect-free sample image pixel by pixel. The method requires a large amount of computation and is not suitable for online implementation. The BB method considers the patterned fabrics as consisting of many rows (columns), and the pattern is designed along each row (column). The weakness of this method is that it cannot detect defects with a size smaller than one repetitive unit, and it is sensitive to cases with a sizable contrast between defective regions and background patterns. The RB method enhances the defective regions with calculations of moving averages and standard deviations. However, this method is unable to detect defects on the borders of an image because of the definition of RB. The TMPM method utilizes a golden image-like approach to exploit a discrepancy measure as a fitness function to detect defects among patterned textures. The pattern matching and subtraction method perform a point-to-point comparison, which is inherently sensitive to noise, misalignment and distortion, etc. The hash function method uses the offset properties of defect-free and regular patterns to detect defects, it is sensitive to noise, but also it cannot outline the shape of any defects after segmentation. In the ER method, detecting fabric defects is similar to conducting fair matches in the spirit of good sportsmanship. However, this method relies on partition size and the number of randomly located partitions. The GHOG and low-rank recovery method utilize the GHOG feature descriptor which is orientation aware, and can detect star- and box-patterned fabric defect images, while it is not satisfactory for dot-patterned fabrics because it lacks distinctive orientation awareness.

The biological vision system can quickly locate salient objects among the background. The normal fabric texture is homogeneous, and the defects are salient among the normal background. Combined with the biological visual perception system, fabric defect detection has become an important research topic. Recently, Guan *et al.* [8] proposed a saliency model using wavelet transform and 'center-surround' contrast technology to highlight the defective regions. However, this method is not suitable for fabric images with complex textures because even in normal regions, the output of 'center-surround' contrast has a higher saliency degree. Guan [31] utilized bottom-up visual attention to generate an overall saliency map to pop out fabric defects and adopted target feature driven (task driven) top-down visual attention to form regions of interest (ROIs) of fabric defects. However, the top-down visual attention reduces adaptability. In our previous work, we have proposed several saliency models based on context analysis and sparse representation to detect defects [7], [32], [33]. These proposed methods have achieved excellent detection results for fabric images with simple textures, but cannot achieved the ideal detection performance for the fabric images with complex texture, especially for the patterned images. Therefore, the mechanism of biological visual perception must be further studied, and a defect detection method with higher accuracy and adaptability for all types of fabric defect images must be proposed.

III. PROPOSED METHOD

Current fabric defect detection methods lack adaptability, and their detection results are not ideal. The biological vision system can quickly locate salient objects among a complex background. Therefore, we propose a novel fabric defect detection method based on a biological vision modeling by simulating the biological vision processing mechanism. First, we adopt the feature descriptor proposed in our previous work, which is generated by modeling retinal ganglion cells and can be used to efficiently characterize all types of fabric images. Then, low-rank representation is utilized to model visual saliency and to identify defective regions. Finally, threshold segmentation is adopted to locate the defective regions. In this section, we discuss our proposed method, which includes four parts: 1) fabric image representations based on biological vision modeling; 2) low-rank representation model construction; 3) optimization of the model; and 4) saliency map generation and segmentation.

A. FABRIC IMAGE REPRESENTATION BASED ON BIOLOGICAL VISION MODELING

Considerable progress has been made in visual perception mechanism research, which has been demonstrated that invariant feature extraction is one of the most important information processing tasks for the human visual system, and is also a common characteristic of senior cortex cells in the process of information integration. Therefore, feature descriptors based on the mechanisms of the human visual system are suitable for characterizing complex textures of all types of fabric images. In our previous work, we proposed an image representation descriptor based on the coding of retinal ganglion cells denoted DERF, and it is highly distinctive, robust, and efficient [9]. In this paper, we adopt this descriptor to characterize all types of fabric images. The descriptor includes difference of Gaussian (DoG) filtering and convolved gradient orientation map sampling. The specific descriptions are as follows:

First, the convolved gradient orientation maps G of the test image I are generated by the DoG method as follows:

$$G_o = \left(\frac{\partial I}{\partial o}\right)^+, \quad 1 \le o \le H \tag{1}$$

where o is the orientation of the derivative, H is the number of orientations, and $(\cdot)^+$ is a nonnegative operator such that $(a)^+ = \max(a, 0)$. Each gradient orientation map is convolved $S+1$ times with Gaussian kernels of different scales to generate Gaussian convolution orientation maps as follows:

$$G_o^{\Sigma} = G_{\Sigma} * \left(\frac{\partial I}{\partial o}\right)^+ \tag{2}$$

where G_{Σ} is a Gaussian kernel with the scale Σ. Different Σ scales correspond to different sizes of convolution regions. For each generated orientation map, the final DoG-convolved gradient orientation maps are generated by subtracting the latter from the former for each pair of neighboring Gaussian convolution orientation maps as follows:

$$D_o^{\Sigma_1} = G_o^{\Sigma_1} - G_o^{\Sigma_2} \; with \; \Sigma_2 > \Sigma_1 \tag{3}$$

After obtaining the DoG-convolved gradient orientation maps, we sample these maps to construct the DERF descriptor by mimicking the structure of receptive fields of P ganglion cells in the range of $0° - 15°$ on the eccentricity of the retina. These sampling points of the descriptor are located in many concentric rings with different radii that increase in an exponential manner. In this paper, we extract the DERF descriptor of S (5) scales and T (8) orientations for each ring, i.e., 5 concentric rings and 8 circles for each ring. The sampling points are evenly distributed on these concentric circles centered on the center point of an image block, and the number of DoG filters is proportional to the radii of these circles; i.e., $\sigma_i = \eta \cdot r_i$. We define $h_{\Sigma}(\xi_0, \nu_0)$ as the vector generated by the values at the position (ξ_0, ν_0) with the same scale Σ in the DoG convolution orientation maps.

$$h_{\Sigma}(\xi_0, \nu_0) = [D_1^{\Sigma}(\xi_0, \nu_0), \cdots D_i^{\Sigma}(\xi_0, \nu_0), \cdots D_H^{\Sigma}(\xi_0, \nu_0)] \tag{4}$$

where D_i^{Σ} represents the DoG convolution orientation map with different orientations and the same scale. Let S denotes the number of layers and T represents the number of sampling orientations for each ring. Finally, the descriptor with the interest point at location (ξ_0, ν_0) can be defined as the concatenation of h vectors:

$$\begin{aligned} &D(\xi_0, \nu_0) \\ &\quad = [h_{\sum_1}(\xi_0, \nu_0), \\ &\qquad h_{\sum_1}(l_1(\xi_0, \nu_0, R_1)), \cdots, h_{\sum_1}(l_T(\xi_0, \nu_0, R_1)) \\ &\qquad h_{\sum_2}(l_1(\xi_0, \nu_0, R_2)), \cdots, h_{\sum_2}(l_T(\xi_0, \nu_0, R_2)) \\ &\qquad\quad \vdots \\ &\qquad h_{\sum_S}(l_1(\xi_0, \nu_0, R_S)), \cdots, h_{\sum_S}(l_T(\xi_0, \nu_0, R_S))]^T \end{aligned} \tag{5}$$

where $l_i(\xi_0, \nu_0, R)$ indicates the location with distance R from (ξ_0, ν_0) in the i-th orientation.

To further improve the characterization ability of the descriptor for fabric images, we utilize the characteristic that the size of the receptive field of ganglion cells can be adjusted dynamically to a certain extent [34] to obtain the DERF descriptor in multi-scale cases. During the process of descriptor extraction, we add two neighboring scales for each sampling point in the single descriptor. The two newly added scales are from the $S(5)$ scales in the single-scale case, and adjacent to the natural scale with the point of interest, one of the scales is greater than the natural scale, while the other is smaller than the nature scale. The DERF descriptor of the multi-scale case $D(\xi_0, \nu_0)$ centered at location (ξ_0, ν_0) is defined as follows:

$$\begin{aligned} &D(\xi_0, \nu_0) \\ &\quad = [h_{\sum_1}(\xi_0, \nu_0), h_{\sum_2}(\xi_0, \nu_0), \\ &\qquad h_{\sum_1}(l_1(\xi_0, \nu_0, R_1)), h_{\sum_2}(l_1(\xi_0, \nu_0, R_1)), \ldots, \\ &\qquad h_{\sum_1}(l_T(\xi_0, \nu_0, R_1)), h_{\sum_2}(l_T(\xi_0, \nu_0, R_1)); \\ &\qquad h_{\sum_1}(l_1(\xi_0, \nu_0, R_2)), h_{\sum_2}(l_1(\xi_0, \nu_0, R_2)), \\ &\qquad h_{\sum_3}(l_1(\xi_0, \nu_0, R_2)), \ldots, h_{\sum_1}(l_T(\xi_0, \nu_0, R_2)), \\ &\qquad h_{\sum_2}(l_T(\xi_0, \nu_0, R_2)), h_{\sum_3}(l_T(\xi_0, \nu_0, R_2)); \\ &\qquad\quad \vdots \\ &\qquad h_{\sum_{S-1}}(l_1(\xi_0, \nu_0, R_S)), h_{\sum_S}(l_1(\xi_0, \nu_0, R_S)), \ldots, \\ &\qquad h_{\sum_{S-1}}(l_T(\xi_0, \nu_0, R_S)), h_{\sum_S}(l_T(\xi_0, \nu_0, R_S));]^T \end{aligned} \tag{6}$$

To achieve the task of fabric defect detection, the test fabric image is uniformly partitioned into image blocks $\{I_i\}_{i=1,2\ldots N}$ with the same size of $m \times m$, where N represents the number of image blocks. For each block, the feature vector $D_i(\xi_0, \nu_0)$ is generated as above. To improve efficiency while maintaining highly distinctive features, principal component analysis (PCA) technology is utilized to reduce the dimensions. We generate P dimension feature vector $f_i, i = 1, 2, \ldots, N$ after dimension reduction by PCA. Then, the feature matrix $F = [f_1, f_2, \ldots, f_N], F \in \mathbb{R}^{P \times N}$ is generated by assembling the feature vectors of all image blocks to represent the test fabric image, where K represents the dimension of the feature vector.

B. LOW-RANK REPRESENTATION MODEL CONSTRUCTION

The low-rank decomposition model is similar to the low-rank and sparsity characteristics of the biological vision system, and it can decompose a given image into low-rank elements that correspond to the background and sparse elements which correspond to the salient object. Even if the fabric texture is complex and diverse, the background is homogeneous and has great redundancy, whereas defective regions are salient. Therefore, the low-rank decomposition model can better deal with the task of fabric defect detection.

A given feature matrix F can be decomposed into a low-rank matrix and a sparse matrix by optimizing the following problem:

$$\min_{(L,S)} \; rank(L) + \gamma \|S\|_0 \quad s.t. \; F = L + S \tag{7}$$

where L and S indicate the low-rank and sparse elements, respectively, and γ is a weighting parameter.

However, the above optimization problem is NP-hard and therefore intractable. Thus, a convex surrogate is as follows:

$$\min_{(L,S)} \|L\|_* + \gamma \|S\|_1 \quad s.t.\ F = L + S \tag{8}$$

where $\|\cdot\|_*$ denotes the nuclear norm of a matrix and is defined as the sum of the singular values of the matrix, and $\|\cdot\|_1$ denotes the ℓ_1 -norm and is defined as the sum of the absolute value of all entries.

During fabric defect detection, defects account for only a small proportion of the entire image; thus, only a small fraction of blocks are salient. From this perspective, the salient defects should be different from the normal background blocks. A strong correlation is usually observed among the feature vectors of normal background blocks, which indicates that the background blocks are self-represented, whereas the defects in the repeated patterns are different from the texture of the background blocks. This finding suggests a more general rank minimization problem [35]:

$$\min_{(Z,S)} \|Z\|_* + \gamma \|S\|_{2,1} \quad s.t.\ F = FZ + S \tag{9}$$

where Z denotes the reconstruction coefficients matrix, which should present a low-rank property; $\|\cdot\|_{2,1}$ indicates the $\ell_{2,1}$-norm and is defined as the sum of ℓ_2 norms of the columns of a matrix:

$$\|S\|_{2,1} = \sum_i \sqrt{\sum_j (S(j,i))^2} \tag{10}$$

where $S(j, i)$ is the (j, i)-th entry of the matrix S because the minimization of $\ell_{2,1}$-norm encourages the columns of S to be zero, which fits our fabric defect detection task well.

Although we directly adopt the low-rank representation model of Eq. (9) to detect defects, the detection results may be contaminated by noise, and the model cannot detect defects that have small differences in the background. To address the first problem mentioned above, the recently proposed image denoising method K-SVD (K-means singular vector decomposition) dictionary learning method is adopted. The K-SVD dictionary learning method was first proposed by Aharon et al. [36] and can effectively suppress additive Gaussian white noises and better retain certain edge and texture information, especially for fabric defect images. Therefore, we utilize the K-SVD method to learn a relatively clean dictionary D, which is a dictionary that linearly spans the data space. The quality of D will influence the discrimination of the representation; therefore, Eq. (9) can be formulated as follows:

$$\min_{(L,S)} \|Z\|_* + \gamma \|S\|_{2,1} \quad s.t.\ F = DZ + S \tag{11}$$

The specific procedure of K-SVD is as follows: For a given fabric image, we partition it into N image blocks with the same size of $\sqrt{m} \times \sqrt{m}$ (m is a number whose square root can be solved), convert the image block into a row vector with size of $m \times 1$, and then stack all of these m row vectors into a matrix $Y_{train} = [Y_1, Y_2, \ldots, Y_N]$, $Y_i \in \mathbb{R}^{m\times 1}$ as the training set. Based on the feature matrix Y, the problem of K-SVD dictionary learning can be considered a joint optimization problem to iteratively update the dictionary D and the sparse coefficient α, and it can be described as follows:

$$\min_{D,\alpha} \|Y_{train} - D\alpha\|_2^2 \quad s.t.\ \forall i, \|\alpha_i\| \le \varepsilon \tag{12}$$

On the other hand, if the texture of the fabric image is complex, or the difference between the defects and background is not obvious, then the low-rank part will be highly correlated with the sparse part. Therefore, when the background is cluttered or has a similar appearance with the defective regions, previous LRR based methods cannot easily separate them. To address this issue, we introduce a Laplacian interactive regularization [37] to enlarge the distance between the subspaces drawn from the low-rank part and sparse part. We define the Laplacian interactive regularization as follows:

$$\Theta(Z, S) = \frac{1}{2} \sum_{i,j=1}^{N} \left\|z_i - z_j\right\|_2^2 \omega_{i,j} = Tr(ZM_F Z^T) \tag{13}$$

where z_i denotes the i-th column of the coefficient matrix Z; $\omega_{i,j}$ denotes the (i, j)-th entry of an affinity matrix, which represents the feature similarity of image blocks ; $Tr(\cdot)$ is the trace of a matrix; and $M_F \in \mathbb{R}^{N\times N}$ represents a Laplacian matrix. The affinity matrix W is defined as follows:

$$\omega_{i,j} = \begin{cases} \exp\left(-\frac{\|f_i - f_j\|^2}{2\sigma^2}\right), & if\ (I_i, I_j) \in \mathbb{V} \\ 0 & otherwise \end{cases} \tag{14}$$

where $\mathbb{V}$ represents the set of adjacent block pairs, which are either neighbors (first-order) or "neighbors of neighbors" (second-order reachable) of the image. The (i, j)-th entry of the Laplacian matrix M_F is as follows:

$$(M_F)_{i,j} = \begin{cases} -\omega_{i,j}, & if\ i \ne j \\ \sum_{j\ne i} \omega_{i,j}, & otherwise \end{cases} \tag{15}$$

Laplacian regularization can increase the distance between feature subspaces by smoothing the vectors in the coefficient matrix according to the local neighborhood derived from the feature matrix F. This approach encourages blocks with similar pixels to share similar or identical representations and encourages blocks with different pixels to have different representations.

We improve on the previous LRR model by introducing K-SVD dictionary learning and Laplacian regularization, to deal with the special task of fabric defect detection. The specific model is described as follows:

$$\begin{aligned} &\min_{Z,S} \|Z\|_* + \lambda \|Z\|_1 + \beta\Theta(Z, S) + \gamma \|S\|_{2,1} \\ &s.t.\ F = DZ + S, Z \ge 0 \end{aligned} \tag{16}$$

where Z represents the coefficient matrix of the dictionary projected into the low-rank space, and its coefficients can well characterize the local similarity between feature vectors;

the second term is a sparse constraint on the coefficient matrix to retain the local similarity of feature vectors; $\Theta(\cdot)$ denotes a Laplacian interactive regularization term to enlarge the distance between the subspace of the low-rank part and sparse part; and λ, β, γ are all trade-off parameters of the model that represent the balance between the coefficient matrix sparsity constraint term, Laplacian interactive regularization term, defect sparsity regularization term and the subspace with the properties of low-rankness, which are positive constants.

To facilitate the solution of the convex optimization problem, we introduce an auxiliary variable J to make the objective function separable; thus, Eq. (16) can be rewritten as follows:

$$\begin{aligned} &\min_{Z,S} \ \|Z\|_* + \lambda \|J\|_1 + \beta Tr(ZM_F Z^T) + \gamma \|S\|_{2,1} \\ &s.t.\ F = DZ + S, Z = J, Z \geq 0 \end{aligned} \tag{17}$$

C. OPTIMIZATION OF THE MODEL

Several algorithms have been proposed for solving LRR optimization problems [38-40]. The alternating direction method of multipliers (ADMM) has attracted considerable attention [41]. ADMM updates the variables by minimizing the augmented Lagrange function in a Gauss-Seidel manner. However, if we directly apply ADMM to solve the problem of Eq. (16), it will result in certain problems as follows:

$$\min_{Z} \ \|Z\|_* + \frac{\lambda}{2} \|\mathcal{C}(Z) - X\|_F^2 \tag{18}$$

where $\mathcal{C}$ denotes a linear mapping, and $\|\cdot\|_F$ represents the Frobenius norm defined as the sum of all the entries of a matrix. If $\mathcal{C}$ is the identity mapping, then Eq. (18) has a closed solution [42]; however, if $\mathcal{C}$ is not the identity mapping, then Eq. (18) can only be solved iteratively.

To remedy the issue above issues and consider the balance between efficiency and accuracy, we resort the linearized alternating direction method with adaptive penalty (LADMAP) [43] to solve the problem defined in Eq. (17). The Lagrange function of Eq. (17) is as follows:

$$\begin{aligned} &L(Z, J, S, D, Y_1, Y_2, \mu) \\ &\quad = \|Z\|_* + \lambda \|J\|_1 \\ &\qquad + \beta Tr\left(ZM_F Z^T\right) + \gamma \|S\|_1 \\ &\qquad + \langle Y_1, F - DZ - S\rangle + \langle Y_2, Z - J\rangle \\ &\qquad + \frac{\mu}{2}\left(\|F - DZ - S\|_F^2 + \|Z - J\|_F^2\right) \end{aligned} \tag{19}$$

where Y_1 and Y_2 are the Lagrange multipliers, and $\mu > 0$ controls the penalty for violating the linear constraints. The optimization problem can be solved by updating the variables by minimizing the Lagrange function and keeping the other variables fixed. The detailed algorithm is shown in Algorithm 1, and its optimization steps are as follows:

1) Update Z_{k+1} by fixing the other variables:

$$\min_{Z} \ \|Z\|_* + \left\langle \nabla_{Z_k} q(Z_k), Z - Z_k \right\rangle + \frac{\eta\mu_k}{2} \|Z - Z_k\|^2 \tag{20}$$

Algorithm 1 Optimization of LRR via LADMAP

Input: feature matrix F, Laplacian matrix M_F and regularization parameters λ, β, γ
Initialization:
$Z_0 = S_0 = J_0 = Y_1^0 = Y_2^0 = 0$, $\rho_0 = 2.5$,
$\mu_0 = 10^{-6}$, $\mu_{max} = 10^{-6}$,
$\varepsilon = 10^{-2}$, $\eta = 1.25 \times \|F\|^2$
While not converged (k=0,1,) do
1) Update Z_{k+1} via Eq. (20).
2) Update J_{k+1} via Eq. (21).
3) Update S_{k+1} via Eq. (22).
4) Update Lagrange multipliers Y_1 and Y_2 via Eq. (23).
5) Update penalty parameter via Eq. (24).
6) Check the convergence condition if
$\|F - DZ_{k+1} - S_{k+1}\| / \|F\| < \varepsilon_1$
or $\mu_{k+1} \cdot max\{\eta \|Z_{k+1} - Z_k\|, \|J_{k+1} - J_k\|, \|S_{k+1} - S_k\|\} < \varepsilon_2$
End while
Output: Z^*,S^*.

where $\nabla_{Z_k} q(Z_k) = \beta\left(Z_k M_F^T + Z_k M_F\right) + \mu_k\left(Z_k - J_k + \frac{Y_2^k}{\mu_k}\right) + \mu_k F^T\left(DZ_k - F + S_k - \frac{Y_1^k}{\mu_k}\right)$. Therefore, $Z_{k+1} = D_{(\eta\mu_k)^{-1}}\left(Z_k - \nabla_{Z_k} q/\eta\right)$, where $D(\cdot)$ represents a singular value thresholding (SVT) operator.

2) Update J_{k+1} by fixing the other variables:

$$J_{k+1} = \max\left\{\mathcal{S}_{\frac{\lambda}{\mu_k}}\left(Z_{k+1} + \frac{1}{\mu_k} Y_2^k\right) 0\right\} \tag{21}$$

where $\mathcal{S}_{\frac{\lambda}{\mu_k}}(\cdot)$ denotes the shrinking operator.

3) Update S_{k+1} by fixing the other variables:

$$S_{k+1} = \mathcal{S}_{\frac{\lambda}{\mu_k}}\left(F - DZ_{k+1} + \frac{1}{\mu_k} Y_1^k\right) \tag{22}$$

4) Update the Lagrange multipliers Y_1 and Y_2:

$$\begin{aligned} Y_1^{k+1} &= Y_1^k + \mu_k (F - DZ_{k+1} - S_{k+1}) \\ Y_2^{k+1} &= Y_2^k + \mu_k (Z_{k+1} - J_{k+1}) \end{aligned} \tag{23}$$

5) Update the penalty parameter μ_{k+1}:

$$\mu_{k+1} = \min(\mu_{\max}, \rho_k \mu_k) \tag{24}$$

where

$$\rho_k = \begin{cases} \rho_0, & \mu_k \cdot \max\{\eta_k \|Z_k - Z_{k-1}\|, \|S_k - S_{k-1}\|\} \leq \xi \\ 1, & otherwise \end{cases} \tag{25}$$

Next, with respect to the fixed Z, J, and S, we update the dictionary D, which is the only variable in the optimization problem of Eq. (19). Thus, Eq. (19) can be written as follows:

$$\begin{aligned} &L(Z, J, S, D, Y_1, Y_2, \mu) \\ &\quad = \langle Y_1, F - DZ - S\rangle \\ &\qquad + \frac{\mu}{2}\|F - DZ - S\|_F^2 + \mathcal{A}(Z, J, S, q) \end{aligned} \tag{26}$$

Algorithm 2 Dictionary Learning Process by ADMM

Input: feature matrix F, and
regularization parameters λ, β, γ
Initialization:
initial dictionary D^0,$\xi_d = 10^{-5}$ **While** not converged $k \leq maxIterD$ do
Update D by fixing the other variables:
$D^{update} = \frac{1}{\mu}\left(Y_1 + \mu\left(F - S\right)\right) Z^T \left(ZZ^T\right)^{-1}$
$D^{k+1} = \alpha D^k + (1-\alpha) D^{update}$
Check the convergence conditions:
$\left\|D^{k+1} - D^k\right\|_\infty < \xi_d$
End while
Output: D.

where $\mathcal{A}(Z, J, S, q)$ is a fixed value. We can derive an optimal dictionary D update immediately:

$$D^{i+1} = \alpha D^i + (1-\alpha) D^{update} \tag{27}$$

where α is a parameter that controls the step of the iteration. The dictionary learning process is summarized as Algorithm 2.

D. SALIENCY MAP GENERATION AND SEGMENTATION

According to the above method, we decompose the feature matrix into a low-rank part that corresponds to the background and sparse part that corresponds to the defect. The corresponding saliency map S is then generated by the sparse matrix S:

$$M(I_i) = \|S(:, i)\|_2^2 = \sum_j (S(j, i))^2 \tag{28}$$

We denoise the saliency map M to obtain a smoothed saliency map $\hat{M}$:

$$\hat{M} = g * (M \circ M) \tag{29}$$

where g is a circular smoothing filter, "$\circ$" indicates the Hadamard inner product operator, and "*" represents the convolution operation.

Next, the saliency map $\hat{M}$ is converted to a grayscale image G:

$$G = \frac{\hat{M} - min\left(\hat{M}\right)}{max\left(\hat{M}\right) - min\left(\hat{M}\right)} \times 255 \tag{30}$$

Finally, G is segmented via an adaptive threshold method [44] to locate the defective regions.

IV. EXPERIMENT

To evaluate the effectiveness of our proposed method, we conduct a series of experiments using two public fabric image databases, and compare the experimental results with State-of-the-Arts.

A. EXPERIMENTAL SETUP

1) FABRIC IMAGE DATABASES

In this paper, we selected two public fabric database for evaluation in our experiment. One is TILDA fabric images dataset [45], which mainly includes plain or twill fabric images with simple textures. It has 3200 defective samples, such as broken ends, holes, multiple netting, thick bars and thin bars.

The other fabric database is from the Research Associate of Industrial Automation Research Laboratory, Department of Electrical and Electronic Engineering, Hong Kong University. It mainly includes the patterned fabric images with complex texture from the star-, box-, dot-patterned fabric database. The star-patterned fabric database contains 30 defect-free and 26 defective images, the box-patterned fabric database contains 25 defect-free and 25 defective images, and the dot-patterned fabric database contains 110 defect-free and 120 defective images.

2) PARAMETER SETTINGS

The parameters in the implementation of our proposed method are set as follows. In fabric image representation, the reduced dimension of feature vector P is set to 64; In low-rank recovery, we empirically set the model parameters λ, β and γ to 0.1, 0.1 and 0.1, and the K of K-SVD to 128, respectively.

All parameters are fixed for all the experiments to demonstrate the robustness and stability of our method. All the resolution of images is 256 pixel 256 pixel,Our test environment is a HP desktop with an Inter(R) Core(TM) i3-2120 3.3 GHZ CPU, and the simulation software is MATLAB 2015a.

B. QUALITATIVE COMPARISON RESULTS

To verify the validity and robustness of the proposed method, we compare our method with other state-of-the-art fabric defect detection methods that include TDVSM [46], PGLSR [47], and LSF-GSA [48]. All of the saliency maps are shown in Fig. 1 - Fig. 4, which show comparisons of plain or twill fabrics, star-patterned fabrics, box-patterned fabrics, and dot-patterned fabrics. In Fig. 1 - Fig. 4, the first row is the original fabric image, and the second to the last rows are saliency maps generated by the TDVSM, PGLSR and LSF-GSA methods and our proposed method.

The TDVSM method generates saliency maps by comparing the texture difference between defects and backgrounds. The method is effective for plain or twill fabrics with simple textures or large texture differences between defects and backgrounds. However, the method is less effective for patterned fabrics with complex textures or limited differences between defects and backgrounds as is shown in the second rows of Fig. 2 - Fig. 4. The PGLSR method detects fabric defects by utilizing the local features learned by the image itself, and it is effective for most fabric images and can locate the position of defective regions. However, this method cannot completely outline the specific shape of defects, espe-

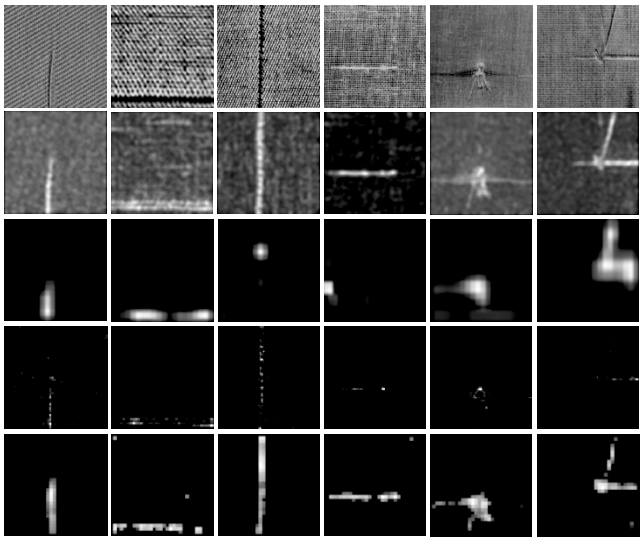

FIGURE 1. Comparison of the saliency map for plain or twill fabrics: (1st row): original images; (2nd row): TDVSM; (3th row): PGLSR; (4th row): LSF-GSA; and (last row): Ours.

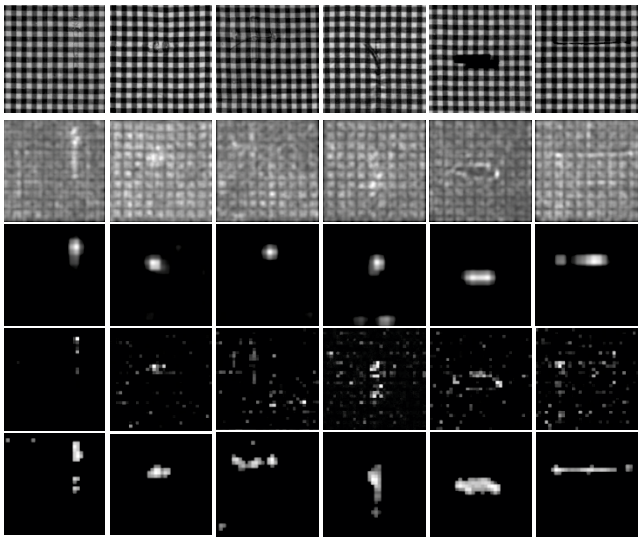

FIGURE 3. Comparison of the saliency map for box-patterned fabrics. ; (1st row): original images; (2nd row): TDVSM; (3th row): PGLSR; (4th row): LSF-GSA; and (last row): Ours.

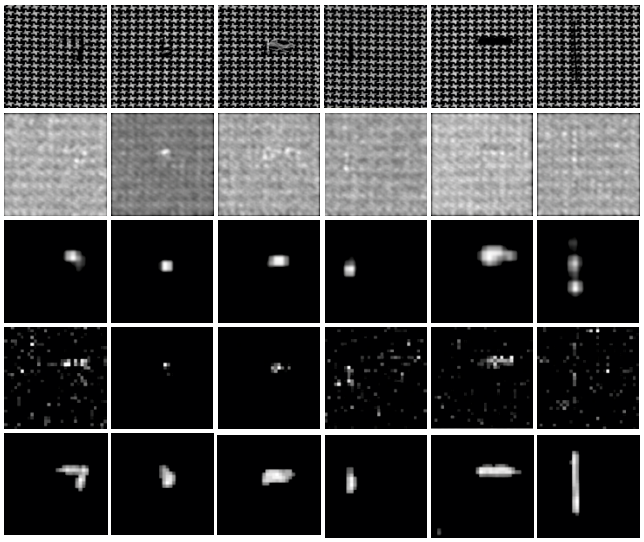

FIGURE 2. Comparison of the saliency map for star-patterned fabrics. ; (1st row): original images; (2nd row): TDVSM; (3th row): PGLSR; (4th row): LSF-GSA; and (last row): Ours.

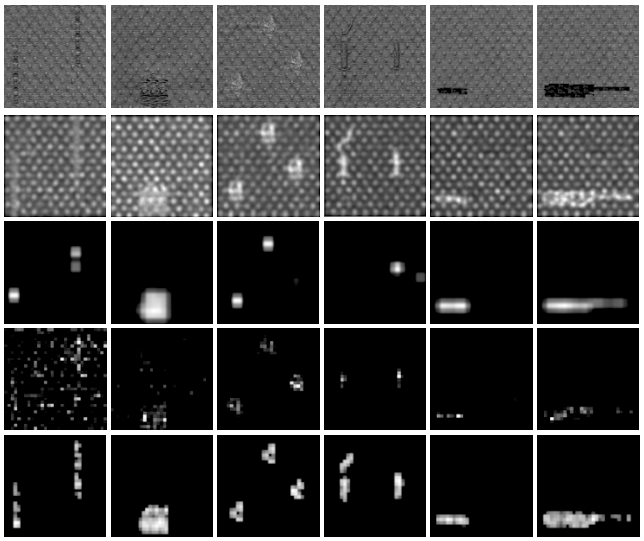

FIGURE 4. Comparison of the saliency map for dot-patterned fabrics. ; (1st row): original images; (2nd row): TDVSM; (3th row): PGLSR; (4th row): LSF-GSA; and (last row): Ours.

cially for broken end defects. The LSF-GSA method detects fabric defects using local features and the overall irregularity of the image, and the method relies on the selected blocks to a certain extent and can detect defects; however, the results always contain noise, which leads to unsatisfactory detection results. The saliency map generated by our proposed method highlights the position of defective regions and outlines the shape of defects for all types of fabric images.

To further demonstrate the effectiveness and accuracy of our proposed method, an improved adaptive threshold segmentation method is utilized to segment the generated saliency map in order to obtain the final detection results, and then the results are compared with the results of other methods as shown in Fig. 5 - Fig. 8 (comparison of plain or twill fabrics, star-patterned fabrics, box-patterned fabrics, and dot-patterned fabrics). The previous analysis that the TDVSM method is not suitable for patterned fabric defect detection. Therefore, the TDVSM method is not adopted in Fig. 6 - Fig. 8. In Fig. 5, the first row is the original fabric images, and the second to the last rows show the detection results by the TDVSM, PGLSR and LSF-GSA methods and our proposed method. In Fig. 6 - Fig. 8, the first row is the original fabric image, the second to the fourth rows are the detection results based on the PGLSR and LSF-GSA method and our method, and the last row is the binary ground-truth images. As shown in Fig. 6 - Fig. 8, our proposed method can

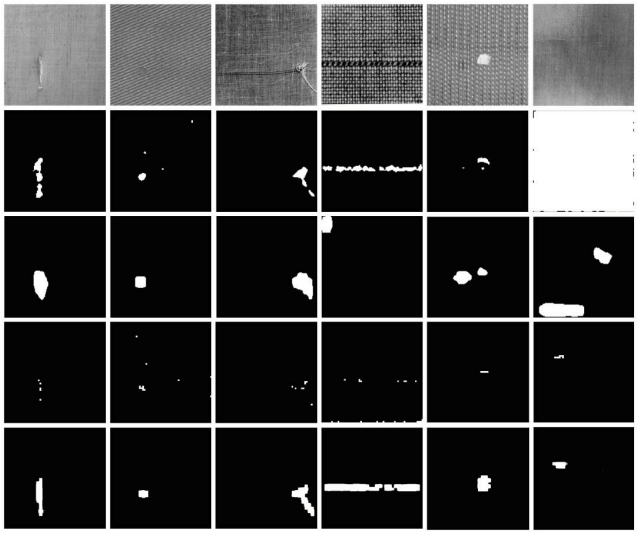

FIGURE 5. Comparison of the detection results for plain or twill fabrics. (1st row): original images; (2nd row): TDVSM; (3rd row): PGLSR; (4th row): LSF-GSA; and (Last row): Ours.

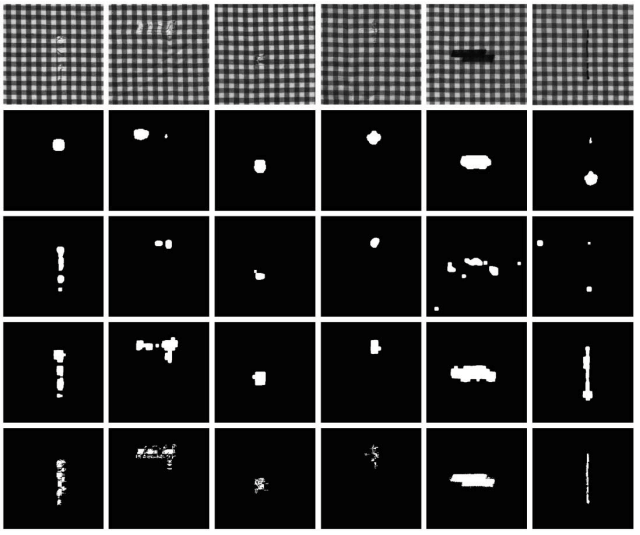

FIGURE 7. Comparison of the detection results for box-patterned fabrics. (1st row): original images; (2nd row): PGLSR; (3rd row): LSF-GSA; (4th row): Ours; and (Last row):GT images.

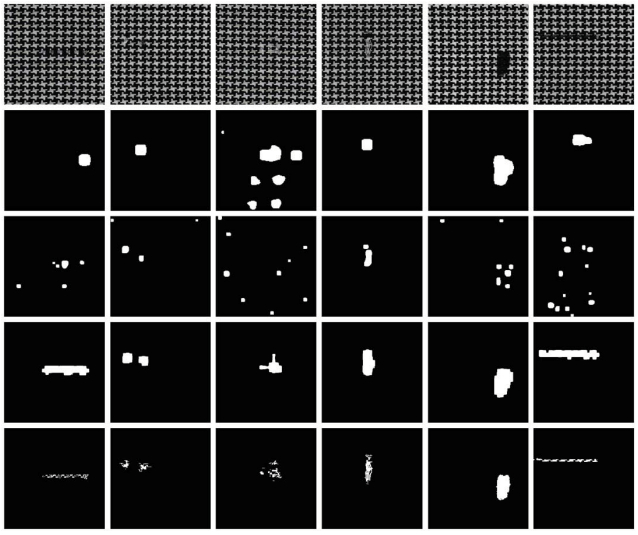

FIGURE 6. Comparison of the detection results for star-patterned fabrics. (1st row): original images; (2nd row): PGLSR; (3rd row): LSF-GSA; (4th row): Ours; and (Last row):GT images.

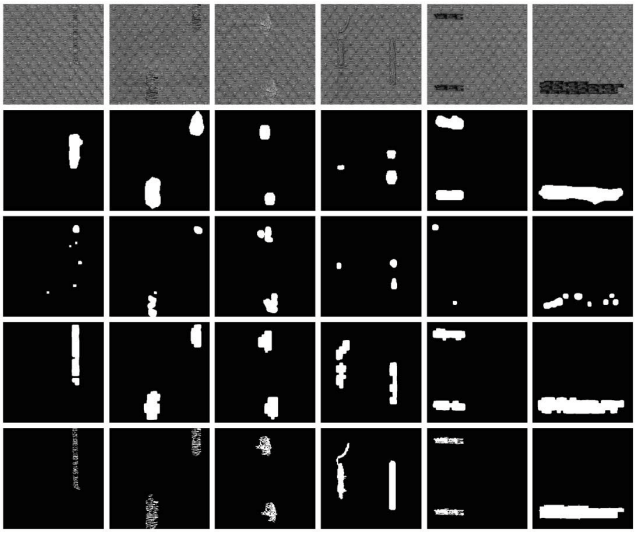

FIGURE 8. Comparison of the detection results for dot-patterned fabrics. (1st row): original images; (2nd row): PGLSR; (3rd row): LSF-GSA; (4th row): Ours; and (Last row):GT images.

better locate the position of defective regions and outline the shape of defects.

C. QUANTITATIVE EVALUATIONS

To perform a comprehensive evaluation, we use several metrics, including the receiver operating characteristic (ROC) curve, precision-recall (PR) curve, and the F-measure curve. These performance metrics are calculated in terms of true positive (TP), true negative (TN), false positive (FP), and false negative (FN), where true positive is the number of defective periodic blocks identified as defective, true negative is the number of defect-free periodic blocks identified as defect-free, false positive is the number of defect-free blocks identified as defective, false negative is the number of defective blocks identified as defect-free. Because of the lack of GT images in the TILDA fabric database, we only presented the quantitative evaluation for the patterned fabric databases. We compared our method with the TDVSM, PGLSR, and LSF-GSA fabric defect detection methods. The ROC curve generated from true positive rates and false positive rates is as shown in Fig. 9. The true positive rate (TPR) and false positive rate (FPR) are defined as follows:

$$TPR = \frac{TP}{TP + FN} \tag{31}$$

$$FPR = \frac{FP}{FP + TN} \tag{32}$$

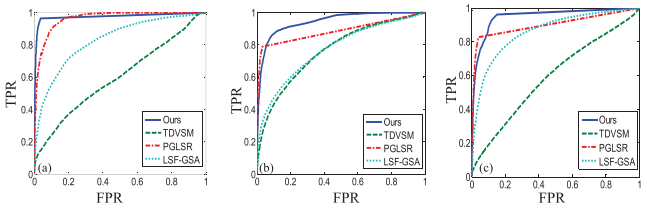

FIGURE 9. Comparison of the ROC curves for (a) star-patterned, (b) box-patterned, and (c) dot-patterned fabrics.

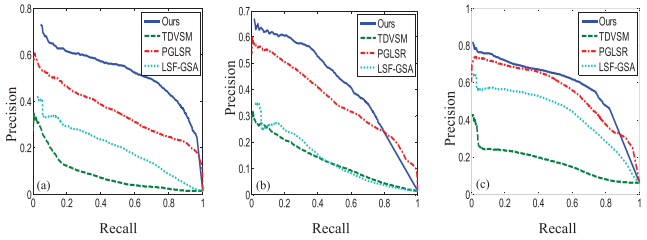

FIGURE 10. Comparison of the PR curves for (a) star-patterned, (b) box-patterned, and (c) dot-patterned fabrics.

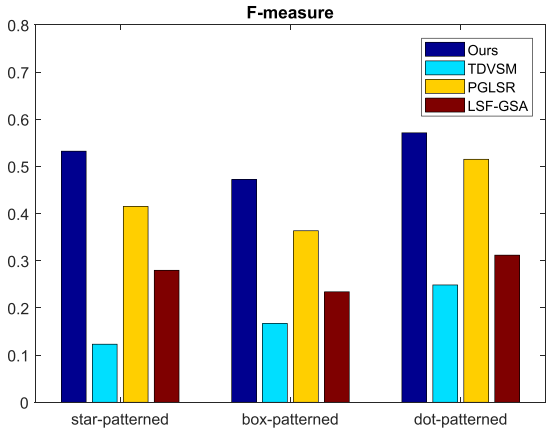

FIGURE 11. Comparison of the F-measure for (a) star-patterned, (b) box-patterned, (c) dot-patterned fabrics.

Fig. 9 (a-c) represents the ROC curve comparisons of star-, box-, and dot-patterned fabrics, and it shows that our proposed method performs better than the other three state-of-the-art methods for the three patterned fabric databases.

To obtain an accurate evaluation of the proposed method, the criteria of *precision* and *recall* are also employed:

$$precision = \frac{TP}{TP + FP} \tag{33}$$

$$recall = \frac{TP}{TP + FN} \tag{34}$$

As is shown in Fig. 10, our proposed method has the highest rate of recall and presents a balanced performance with respect to precision. In addition, the F-measure is adopted by taking both precision and recall into account as shown in Fig. 11, which demonstrates the effectiveness, robustness and superiority of our proposed method.

$$F = 2\frac{precision \cdot recall}{precision + recall} \tag{35}$$

D. TIMING SPENT ANALYSIS

In this paper, LADMAP instead of ADMM is adopted to solve the constructed model for improving the efficiency of the proposed method. In order to verify its efficiency, we test the timing spent for the two methods. For ADMM solution, the spent time is 0.56 s for detecting one image in our simulation environment; otherwise, the spent time for the LADMAP solution method is 0.23 s. Therefore, our improved method can efficiently reduce the spent time, thus it is helpful for the real-time inspection demands.

V. CONCLUSION

In this paper, we propose a novel fabric defect detection method based on biological vision modeling and low-rank representation by simulating biological vision, which has the ability to quickly locate salient objects. The main features of our method are summarized as follows. 1) Inspired by the hierarchical information processing of the biological visual system, which can quickly locate the salient object, we establish a fabric defect detection framework by modeling the biological vision. The descriptor based on coding retinal ganglion cells is used to characterize all types of fabric textures; and low-rank representation is adopted to model visual saliency. 2) Dictionary learning is integrated into the low-rank representation model to denoise the saliency map. 3) A Laplacian regularization term is integrated into the low-rank representation model to enlarge the gaps between the defect region and the background. 4) In order to improve the efficiency of the proposed method, LADMAP instead of ADMM is adopted to solve the constructed model.

We also compare the performance of the proposed approach with that of previous approaches, such as the WT, TDVSM, PGLSR, and LSF-GSA methods. The qualitative and quantitative experimental results demonstrate that our proposed method is more effective, robust and adaptable than other state-of-the-art methods for plain and twill fabrics with simple textures as well as for patterned fabrics with complex textures. In addition, the proposed method provides a new solution for detecting surface defects of other industrial products.

ACKNOWLEDGMENT

The authors would like to thank Dr. H. Y. T. Ngan, Industrial Automation Research Laboratory, Department of Electrical and Electronic Engineering, The University of Hong Kong, for providing the database of patterned fabric images.

REFERENCES

[1] M. Shi, R. Fu, S. Bai, B. Xu, and Y. Guo, "Fabric defect detection using local contrast deviations," *Multimedia Tools Appl.*, vol. 52, no. 1, pp. 147–157, 2011.

[2] M. Li, S. Cui, and Z. Xie, "Application of Gaussian mixture model on defect detection of print fabric," *J. Textile Res.*, vol. 36, no. 8, pp. 94–98, 2015.

[3] A. S. Tolba, "Fast defect detection in homogeneous flat surface products," *Expert Syst. Appl.*, vol. 38, no. 10, pp. 12339–12347, 2011.

[4] Z. Liu, L. Yan, C. Dong, Y. Li, and C. Li, "Fabric defect detection algorithm based on sparse optimization," *J. Textile Res.*, vol. 37, no. 5, pp. 56–63, 2016.

[5] H. Y. T. Ngan, G. K. H. Pang, and S. P. Yung, "Wavelet based methods on patterned fabric defect detection," *Pattern Recognit.*, vol. 38, no. 4, pp. 559–576, 2005.

[6] C. S. C. Tsang, H. Y. T. Ngan, and G. K. H. Pang, "Fabric inspection based on the Elo rating method," *Pattern Recognit.*, vol. 51, pp. 378–394, Mar. 2016.

[7] Z. Liu, C. Li, and Q. Zhao, "A fabric defect detection algorithm via context-based local texture saliency analysis," *Int. J. Clothing Sci. Technol.*, vol. 27, no. 5, pp. 738–750, 2015.

[8] S. Guan, Z. Gao, N. Xu, and N. Wu, "Defect detection of plain weave based on visual saliency mechanism," *J. Textile Res.*, vol. 35, no. 4, pp. 56–61, 2014.

[9] D. Weng, Y. Wang, M. Gong, D. Tao, H. Wei, and D. Huang, "DERF: Distinctive efficient robust features from the biological modeling of the P ganglion cells," *IEEE Trans. Image Process.*, vol. 24, no. 8, pp. 2287–2302, Aug. 2015.

[10] J. Yan, J. Liu, Z. Niu, Y. Liu, and Y. Li, "Visual saliency detection via rank-sparsity decomposition," in *Proc. IEEE Int. Conf. Image Process.*, Sep. 2010, pp. 1089–1092.

[11] D. Hong, Z. Pan, and X. Wu, "Improved differential box counting with multi-scale and multi-direction: A new palmprint recognition method," *Optik-Int. J. Light Electron Opt.*, vol. 125, no. 15, pp. 4154–4160, 2014.

[12] W. Bian and Q. Zhu, "The measurement method based on the block adaptive double thresholds of motion target detection," in *Proc. IEEE Int. Conf. Mechatronics Automat.*, Aug. 2015, pp. 82–86.

[13] S. M. Alper, V. Avşar, and H. Özdemir, "Textural fabric defect detection using statistical texture transformations and gradient search," *J. Textile Inst.*, vol. 105, no. 9, pp. 998–1007, 2014.

[14] X. Yang, "Fabric defect detection of statistic aberration feature based on GMRF model," *J. Textile Res.*, vol. 34, no. 4, pp. 137–142, 2013.

[15] M. S. Allili, N. Baaziz, and M. Mejri, "Texture modeling using contourlets and finite mixtures of generalized Gaussian distributions and applications," *IEEE Trans. Multimedia*, vol. 16, no. 3, pp. 772–784, Apr. 2014.

[16] K. Sakhare, A. Kulkarni, N. Kare, and M. Kumbhakarn, "Spectral and spatial domain approach for fabric defect detection and classification," in *Proc. Int. Conf. Ind. Instrum. Control*, 2015, pp. 640–644.

[17] L. Tong, W. K. Wong, and C. K. Kwong, "Differential evolution-based optimal Gabor filter model for fabric inspection," *Neurocomputing*, vol. 173, pp. 1386–1401, Jan. 2016.

[18] Z. Wen, J. Cao, S. Ying, and X. Liu, "Fabric defects detection using adaptive wavelets," *Int. J. Clothing Sci. Technol.*, vol. 26, no. 3, pp. 202–211, 2014.

[19] J. Zhou and J. Wang, "Fabric defect detection using adaptive dictionaries," *Textile Res. J.*, vol. 83, no. 17, pp. 1846–1859, 2013.

[20] T. Qu, L. Zou, X. Chen, C. Fan, and Q. Zhang, "Defect detection on the fabric with complex texture via dual-scale over-complete dictionary," *J. Textile Inst.*, vol. 107, no. 6, pp. 743–756, 2015.

[21] J. Zhou, D. Semenovich, J. Wang, and A. Sowmya, "Dictionary learning framework for fabric defect detection," *J. Textile Inst.*, vol. 105, no. 3, pp. 223–234, 2014.

[22] H. Y. T. Ngan and G. K. H. Pang, "Novel method for patterned fabric inspection using Bollinger bands," *Opt. Eng.*, vol. 45, no. 8, pp. 087202-1–087202-15, 2006.

[23] H. Y. T. Ngan and G. K. H. Pang, "Regularity analysis for patterned texture inspection," *IEEE Trans. Autom. Sci. Eng.*, vol. 6, no. 1, pp. 131–144, Jan. 2009.

[24] G. Stübl, J.-L. Bouchot, B. Moser, and P. Haslinger, "Discrepancy norm as fitness function for defect detection on regularly textured surfaces," in *Pattern Recognition*. Berlin, Germany: Springer, 2012, pp. 428–437.

[25] M. F. M. Costa, F. Rodrigues, and J. Guedes, "Automated evaluation of patterned fabrics for defect detection," in *Proc. Int. Soc. Opt. Photon. Edu. Training Opt. Photon. (ETOP)*, 2000, pp. 403–407.

[26] C. Sanby, L. Norton-Wayne, and R. Harwood, "The automated inspection of lace using machine vision," *Mechatronics*, vol. 5, nos. 2–3, pp. 215–231, 1995.

[27] U. Farooq, T. King, N. Kapur, and P. H. Gaskell, "Machine vision using image data feedback for fault detection in complex deformable Webs," *Trans. Inst. Meas. Control*, vol. 26, no. 2, pp. 119–137, 2004.

[28] J. Cano, J. C. Perez-Cortes, R. Paredes, J. Arlandis, and J. M. Valiente, "Textile inspection with a parallel computer cluster," in *Proc. 5th Int. Conf. Quality Control Artif. Vis. (QCAV)*, Le Creusot, France, 2001, pp. 1–6.

[29] I. C. Baykal, R. Muscedere, and G. A. Jullien, "On the use of hash functions for defect detection in textures for in-camera Web inspection systems," in *Proc. IEEE Int. Symp. Circuits Syst. (ISCAS)*, vol. 5, May 2002, pp. V-665–V-668.

[30] G. Gao, D. Zhang, Z. Liu, Q. Liu, and C. Li, "A novel patterned fabric defect detection algorithm based on GHOG and low-rank recovery," in *Proc. IEEE 13th Int. Conf. Signal Process. (ICSP)*, Nov. 2016, pp. 1118–1123.

[31] S. Guan, "Fabric defect detection using an integrated model of bottom-up and top-down visual attention," *J. Textile Inst.*, vol. 107, no. 2, pp. 215–224, 2015.

[32] C. Li, R. Yang, Z. Liu, G. Gao, and Q. Liu, "Fabric defect detection via learned dictionary-based visual saliency," *Int. J. Clothing Sci. Technol.*, vol. 28, no. 4, pp. 530–542, 2016.

[33] Z. F. Liu, C. L. Li, and S. M. Ding, "A novel fabric defect detection algorithm using sparse representation-based visual saliency," in *Proc. Int. Conf. Artif. Intell. Ind. Appl.*, 2015, pp. 459–466.

[34] Y. Li, H. Li, H.-Q. Gong, P.-J. Liang, and P. M. Zhang, "Characteristics of receptive field encoded by synchronized firing pattern of ganglion cell group," *Acta Biophys. Sin.*, vol. 27, no. 3, pp. 211–221, 2011.

[35] G. Liu, Z. Lin, S. Yan, J. Sun, Y. Yu, and Y. Ma, "Robust recovery of subspace structures by low-rank representation," *IEEE Trans. Pattern Anal. Mach. Intell.*, vol. 35, no. 1, pp. 171–184, Jan. 2013.

[36] M. Aharon, M. Elad, and A. M. Bruckstein, "K-SVD: Design of dictionaries for sparse representation," in *Proc. SPARS*, Rennes, France. 2005, pp. 9–12.

[37] H. Peng, B. Li, H. Ling, W. Hu, W. Xiong, and S. J. Maybank, "Salient object detection via structured matrix decomposition," *IEEE Trans. Pattern Anal. Mach. Intell.*, vol. 39, no. 4, pp. 818–832, Apr. 2017.

[38] M. Chen, A. Ganesh, Z. Lin, Y. Ma, J. Wright, and L. Wu, "Fast convex optimization algorithms for exact recovery of a corrupted low-rank matrix," *J. Marine Biol. Assoc. U.K.*, vol. 56, no. 3, pp. 707–722, Aug. 2009.

[39] M. Tao and X. Yuan, "Recovering low-rank and sparse components of matrices from incomplete and noisy observations," *SIAM J. Optim.*, vol. 21, no. 2, pp. 57–81, 2011.

[40] K.-C. Toh and S. Yun, "An accelerated proximal gradient algorithm for nuclear norm regularized least squares problems," *Pacific J. Optim.*, vol. 6, pp. 615–640, Sep. 2010.

[41] Z. Wen, D. Goldfarb, and W. Yin, "Alternating direction augmented Lagrangian methods for semidefinite programming," *Math. Program. Comput.*, vol. 2, nos. 3–4, pp. 203–230, Dec. 2010.

[42] J.-F. Cai, E. J. Candès, and Z. Shen "A singular value thresholding algorithm for matrix completion," *SIAM J. Optim.*, vol. 20, no. 4, pp. 1956–1982, 2010.

[43] Z. Lin, R. Liu, and Z. Su, "Linearized alternating direction method with adaptive penalty for low-rank representation," in *Proc. Adv. Neural Inf. Process. Syst.*, 2011, pp. 612–620.

[44] L. Zhoufeng, W. Jiuge, Z. Quanjun, and L. Chunlei, "Research on fabric defect detection algorithm based on improved adaptive threshold," *Microcomput. Appl.*, vol. 32, no. 10, pp. 40–44, 2013.

[45] (May 6, 2013). *Workgroup on Texture Analysis of DFG TILDA Textile Texture Database [DB/OL]*. [Online]. Available: http//lmb.informatik.unifreiburg.de/research/dfg-texture/tilda

[46] L. Chunlei, Z. Zhaoxiang, Z. Zhoufeng, L. Liang, and L. Quanjun, "A novel fabric defect detection algorithm based on textural differential visual saliency model," *J. Shandong Univ.*, vol. 44, no. 4, pp. 1–8, 2014.

[47] J. Cao, J. Zhang, N. Wang, X. Liu, and Z. Wen, "Fabric defect inspection using prior knowledge guided least squares regression," *Multimedia Tools Appl.*, vol. 46, pp. 4141–4157, Feb. 2017.

[48] Z. Liu, Q. Zhao, Y. Dong, L. Yan, and C. Li, "Fabric defect detection algorithm using local statistic features and global saliency analysis," *J. Textile Res.*, vol. 35, no. 11, pp. 62–67, 2014.

CHUNLEI LI received the B.S. degree in computer science from Zhengzhou University, China, in 2001, the M.S. degree from Hohai University, China, in 2004, and the Ph.D. degree in computer science from Beihang University, China, in 2012.

He is currently an Associate Professor with the School of Electronics and Information, Zhongyuan University of Technology. In recent years, he published over 50 technical papers and has authored two books. He holds three patents. His research interests include machine vision for fabric defect detection, pattern recognition, and low-rank representation.

GUANGSHUAI GAO received the bachelor's degree in applied physics from the Zhongyuan University of Technology, Zhengzhou, China, in 2014, and the M.S. degree from the School of Electronic and Information Engineering, Zhongyuan University of Technology, in 2017. He is currently pursuing the Ph.D. degree with the Laboratory of Intelligent Recognition and Image Processing, Beijing Key Laboratory of Digital Media, School of Computer Science and Engineering, Beihang University. His research interests include image processing, pattern recognition, and digital machine learning.

ZHOUFENG LIU received the B.S. degree from Lanzhou University, Lanzhou, China, in 1985, and the M.S. and Ph.D. degrees from the Beijing Institute of Technology, Beijing, China, in 1988 and 1994, respectively.

From 1990 to 1995, he was a Lecturer with Zhengzhou University, Zhengzhou, China. From 1998 to 2004, he was an Associate Professor. Since 2004, he has been a Professor with the Zhongyuan University of Technology. He was the Technical Leader and the Consultation Committee Member of Henan Province. His research interests include radar image processing and artificial intelligence.

MIAO YU received the B.B.A. and M.S. degrees from Southwest Jiaotong University in 2004 and 2007, respectively, and the Ph.D. degree from the Institute of Automation, Chinese Academy of Sciences, in 2016. Since 2007, he has been with the Zhongyuan University of Technology, where he is currently a Lecturer. His research interests include parallel computing, probabilistic graphical models, higher order energy minimization, and scene understanding.

DI HUANG received the B.S. and M.S. degrees in computer science from Beihang University, Beijing, China, in 2005 and 2008, respectively, and the Ph.D. degree in computer science from the Ecole Centrale de Lyon, Lyon, France, in 2011. He joined the Laboratory of Intelligent Recognition and Image Processing, Beijing Key Laboratory of Digital Media, School of Computer Science and Engineering, Beihang University, as a Faculty Member. His current research interests include biometrics, in particular, on 2-D/3-D face analysis, image/video processing, and pattern recognition.